

## BRIEF REPORTS

*Brief Reports are short papers which report on completed research or are addenda to papers previously published in the Physical Review. A Brief Report may be no longer than four printed pages and must be accompanied by an abstract.*

Excitation of  $^{123}\text{Te}^m$  and  $^{125}\text{Te}^m$  through  $(\gamma, \gamma')$  reactions

J. J. Carroll, T. W. Sinor, D. G. Richmond, K. N. Taylor, and C. B. Collins

*Center for Quantum Electronics, The University of Texas at Dallas, P. O. Box 830688, Richardson, Texas 75083*

M. Huber, N. Huxel, P. v. Neumann-Cosel, A. Richter, C. Spieler, and W. Ziegler

*Institut für Kernphysik, Technische Hochschule Darmstadt, D-6100 Darmstadt, Germany*

(Received 5 October 1990)

Photoexcitation of the long-lived isomers  $^{123}\text{Te}^m$ ,  $T_{1/2} = 119.7$  d, and  $^{125}\text{Te}^m$ ,  $T_{1/2} = 58$  d, was produced with bremsstrahlung from the superconducting Darmstadt linear accelerator. The excitation function for the reaction  $^{123}\text{Te}(\gamma, \gamma')^{123}\text{Te}^m$  was measured between 2 and 6 MeV. It indicated that the isomer was populated by resonant absorption through isolated intermediate states having integrated cross sections in excess of  $10^{-26}$  cm<sup>2</sup> keV, i.e., values about 100 times larger than most  $(\gamma, \gamma')$  activation reactions reported previously. An excitation function was also obtained for the reaction  $^{125}\text{Te}(\gamma, \gamma')^{125}\text{Te}^m$  in this energy range.

## INTRODUCTION

It has been recently discovered<sup>1</sup> that the reaction  $^{180}\text{Ta}^m(\gamma, \gamma')^{180}\text{Ta}$  occurs with an integrated cross section that is orders of magnitude larger than what could have been reasonably expected. At energies below the threshold for neutron evaporation the photoexcitation of isomers is usually characterized by values of  $10^{-28}$ – $10^{-27}$  cm<sup>2</sup> keV. Although the inverse, deexcitation of an isomer had not been previously observed, there was no *a priori* reason to expect it to be more probable, particularly since the transition requires a spin change of  $\Delta K = 8$ . Of considerable astrophysical significance,<sup>2,3</sup> the result reported for  $^{180}\text{Ta}^m$  approached  $10^{-24}$  cm<sup>2</sup> keV and raised some interesting questions of nuclear structure. It also provided unexpected encouragement of schemes for pumping a  $\gamma$ -ray laser that would depend upon the sudden deexcitation of isomeric populations.<sup>4</sup>

Whether the deexcitation of  $^{180}\text{Ta}^m$  was an isolated example limited to odd-odd nuclei with a high density of states was considered in two subsequent studies. In the first the excitation function for  $^{180}\text{Ta}^m(\gamma, \gamma')^{180}\text{Ta}$  was measured with a bremsstrahlung source by varying the end point of the spectrum. It was found<sup>5</sup> that the  $(\gamma, \gamma')$  reactions of  $^{180}\text{Ta}^m$  occurred for two discrete excitation energies of 2.8 and 3.6 MeV with integrated cross sections of  $1.2 \times 10^{-25}$  and  $3.5 \times 10^{-25}$  cm<sup>2</sup> keV, respectively. The high density of excited nuclear states seemed to play no particular role.

In the second experiment<sup>6</sup> 19 isomers were excited with the bremsstrahlung spectra from four different accelerators. Despite the relatively coarse mesh of energies at which end points could be set between 0.5 and 11 MeV, several isomers were excited through integrated

cross sections that were surprisingly large at 4 MeV. One curiosity was the first report of the photoexcitation of 119.7d,  $^{123}\text{Te}^m$ , the longest-lived isomer ever populated by  $(\gamma, \gamma')$  reactions and one of the candidate nuclides for a  $\gamma$ -ray laser. This is a fairly light nucleus having no particularly high density of states. Also, there is little experimental or theoretical information on electromagnetic transitions between excited levels in  $^{123}\text{Te}$  above 1 MeV.

It was the purpose of the experiment described in this Brief Report to measure the excitation function for both  $^{123}\text{Te}^m$  and  $^{125}\text{Te}^m$ . Exploiting the precision with which the end points of the spectra could be set between 2 and 6 MeV, the  $(\gamma, \gamma')$  reactions were found to occur through relatively few gateways with large integrated cross sections approaching  $10^{-25}$  cm<sup>2</sup> keV.

## EXPERIMENTAL ANALYSIS AND RESULTS

Elemental tellurium samples were used in this study, and all isotopes were present in their natural abundances. Nominal amounts of 17 g were contained in plastic (Delrin) cylinders with outer diameters of 3.8 cm and heights of 1.5 cm. Calibration targets were fashioned from identical containers holding about 2 g of 99.99% pure SrF<sub>2</sub>. Its use in calibrating bremsstrahlung spectra has been recently emphasized.<sup>5,6</sup>

Isomeric populations were produced by exposing the targets to bremsstrahlung from a 3-mm tantalum converter foil irradiated by the electron beam from the injector of the new 130-MeV S-DALINAC at the Technische Hochschule Darmstadt.<sup>7</sup> Electron energies were varied between 2 and 6 MeV with a typical step size of 250 keV. These electron energies were measured with an accuracy of 50 keV before and after each exposure. The diameter

of the beam at the converter, typically 2 mm, was also monitored. At each end point a sample stack of tellurium and strontium was irradiated axially in close proximity to the converter. The proper alignment of the beam was achieved by maximizing the dose delivered to a remote ionization chamber shielded to sample only the central 12 mrad of the bremsstrahlung cone. Variations in all beam parameters were recorded during the experiments. In particular, the charge passed to the converter was determined by digitizing the current and integrating it. Exposures were typically 4 h in duration for a beam current of about  $20 \mu\text{A}$ .

The numbers of isomers produced by these irradiations were determined from the counting rates measured in distinctive fluorescence lines. The transitions responsible for the  $\gamma$ -ray signatures used in these measurements are indicated by bold arrows in the energy-level diagrams of Figs. 1(a) and 1(b).

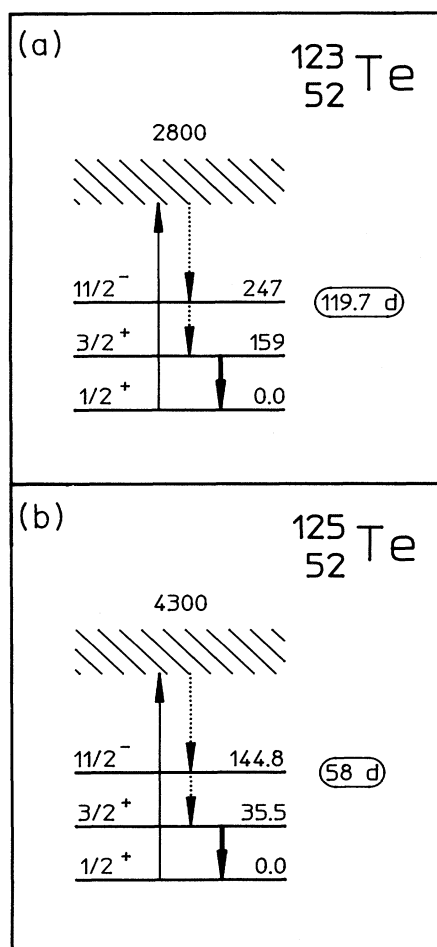


FIG. 1. Schematic energy-level diagrams for (a)  $^{123}\text{Te}$  and (b)  $^{125}\text{Te}$ . Half-lives of the isomers are shown in the ovals, and the energies of the levels shown are given in keV. The bold arrows show the transitions which give rise to distinctive  $\gamma$ -ray emissions measured in this work. The dashed arrows indicate transitions which are not directly observed.

After irradiation the tellurium samples were transported to the Center for Quantum Electronics, University of Texas at Dallas, where high-resolution spectra were collected with an HPGe detector. An example of the data obtained with a 6-MeV exposure is shown in Fig. 2. The fluorescence peak<sup>8</sup> at 159.0 keV from the decay of  $^{123}\text{Te}^m$  is apparent, and even the  $\gamma$  rays from the strongly converted transition of  $^{125}\text{Te}^m$  at 35.5 keV are clearly visible.

Because of the shorter isomeric lifetimes the  $\text{SrF}_2$  calibration, samples<sup>5,6</sup> were counted on site with a Ge(Li) detector to measure the yield of  $^{87}\text{Sr}^m$ . This isomer has a half-life of 2.8 h and a fluorescence signature at 388.4 keV. The raw number of counts in each peak was corrected for the finite durations of exposure and counting, the absolute counting efficiencies of the detectors, and the relative emission intensity. The opacity of the samples to the escape of the signature  $\gamma$  rays was compensated by a factor calculated with a Monte Carlo code for each detector geometry.

The experimentally measured yield of isomers,  $N_f$  resulting from the irradiation of  $N_T$  ground-state nuclei with bremsstrahlung is given analytically by

$$N_f = N_T \int_{E_C}^{E_0} \sigma(E) \frac{d\Phi(E)}{dE} dE, \quad (1)$$

where  $E_0$  is the end-point energy,  $d\Phi(E)/dE$  is the time-integrated spectral intensity in  $\text{cm}^{-2}\text{keV}^{-1}$  of the photon field, and  $\sigma(E)$  is the cross section in  $\text{cm}^2$  for the reaction. The spectral intensity is conveniently expressed as the product of a flux of all photons above a cutoff energy  $E_C$  of 1 MeV,  $\Phi_0$  incident on the target, and a relative intensity function  $F(E, E_0)$ , which is normalized according to

$$\int_{E_C}^{E_0} F(E, E_0) dE = 1. \quad (2)$$

Equation (2) allows the definition of a normalized yield, or activation per photon,  $A_f(E_0)$  given by

$$A_f(E_0) \equiv \frac{N_f}{N_T \Phi_0} = \int_{E_C}^{E_0} \sigma(E) F(E, E_0) dE. \quad (3)$$

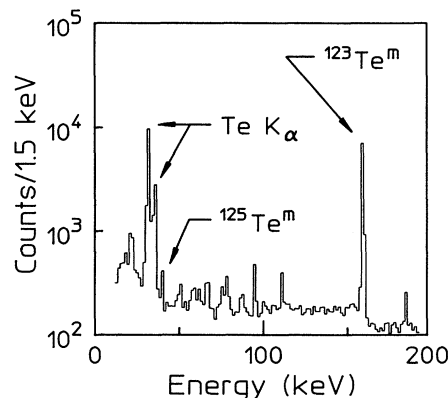


FIG. 2. Pulse-height spectrum obtained from a tellurium sample after a 6-MeV end-point irradiation. Peaks not explicitly marked are due to counting chamber background.

Plots of this quantity as a function of  $E_0$  give the excitation functions for  $^{123}\text{Te}^m$  and  $^{125}\text{Te}^m$  shown in Figs. 3(a) and 3(b). This normalization makes these curves relatively insensitive to variations in isomeric population that occur simply because all the intensities increase when the end point is raised. Instead, their appearance is primarily determined by the density, location, and integrated cross sections of the states mediating the reactions.

Calculated spectra of both  $\Phi_0$  and  $F(E, E_0)$  were obtained from the EGS4 electron-photon transport code developed at SLAC.<sup>9</sup> This Monte Carlo program is well established in the medical physics community, and its general validity has been demonstrated elsewhere.<sup>10,11</sup> In this work confidence in the calculated photon spectra was maintained by calibrating them with the reaction  $^{87}\text{Sr}(\gamma, \gamma')^{87}\text{Sr}^m$  as discussed in Ref. 5.

At energies of interest in these experiments, gateways have widths that are small in comparison to their spacings, and Eq. (3) reduces to a summation, giving

$$A_f(E_0) = \sum_j (\sigma\Gamma)_{fj} F(E_j, E_0), \quad (4)$$

where  $(\sigma\Gamma)_{fj}$  is the integrated cross section and  $E_j$  is the excitation energy of the  $j$ th intermediate state feeding the isomer. It is then possible to define a quantity  $R_M(E_0)$ ,

which represents the residue of activation after subtracting contributions from the  $M$  lowest-lying intermediate states:

$$R_M(E_0) = A_f(E_0) - \sum_{E_j=E_1}^{E_M} (\sigma\Gamma)_{fj}' F(E_j, E_0), \quad (5)$$

where  $E_M$  is the resonance energy of the highest-lying intermediate state contributing. Fitted values of the integrated cross sections  $(\sigma\Gamma)_{fj}'$  were found by minimizing  $R_M(E_0)$  for the lowest-energy state giving a break in the excitation function, and then iterating after including any new gateways suggested by the data. In the case of  $^{87}\text{Sr}$ , the calibration procedures described earlier<sup>5,6</sup> were confirmed in the present work as a test of confidence. This provided experimental validation of the calculated photon spectra as well as confirming the experimental practice.

An identical analysis for  $^{123}\text{Te}^m$  was based upon the excitation function of Fig. 3(a). The pronounced increase in yield beginning near 3 MeV indicates the location of an intermediate state, while the low level of activation below this energy suggests the participation of smaller gateways having  $E_j < 2$  MeV. The number and location of these lower-energy states could not be determined in the current work; nor does the literature provide any information. It was found that a single state near 1 MeV with an integrated cross section of  $(60 \pm 20) \times 10^{-29} \text{ cm}^2 \text{ keV}$  could give the activation observed below 3 MeV, but this assignment is not unique. The possible variations are indicated in Table I and do not significantly contribute to the uncertainties reported for the other gateways. Using this hypothetical state to remove the base-line yield, the residue  $R_1(E_0)$  indicated two strong gateways at 2.8 and 4.2 MeV. The fitted  $(\sigma\Gamma)_{ij}'$  corresponding to these states are given in Table I and are much larger than the base-line state at 1 MeV. These values were determined to within the uncertainties explicitly shown in Table I.

The excitation function obtained for population of  $^{125}\text{Te}^m$  provided less detail, but the data of Fig. 3(b) were still consistent with an intermediate state located between 4.2 and 4.5 MeV, as given in Table I.

Because of the low  $(\gamma, n)$  threshold of the naturally occurring component of the deuterium in the plastic sample containers, it was necessary to evaluate the effects of all neutrons produced in the irradiation environment.

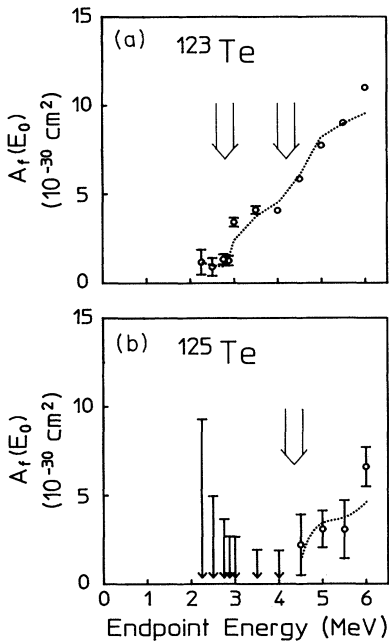


FIG. 3. Linear plots of yield normalized to the flux calculated for a low-energy cutoff of 1 MeV as functions of bremsstrahlung end-point energy for (a)  $^{123}\text{Te}$  and (b)  $^{125}\text{Te}$ . Where no error bars are shown, statistical errors are comparable to the symbol size. Error bars shown without symbols in (b) represent upper bounds on the activation where fluorescence was not observed above the level of background. Dotted curves plot the values calculated from the model of Eq. (4) using the results of Table I. The locations of the gateways determined in this work are indicated by the large arrows whose widths represent the available experimental resolution.

TABLE I. Values of fitted integrated cross sections  $(\sigma\Gamma)_{ij}'$  for gateway states determined from the excitation functions of Figs. 3(a) and 3(b) for the  $(\gamma, \gamma')$  reactions populating the isomers  $^{123}\text{Te}^m$  and  $^{125}\text{Te}^m$ . The gateway excitation energies  $E_j$  for these levels are given at the centroid of the appropriate experimental bins.

Isotope	Gateway energy (MeV)	$(\sigma\Gamma)_{ij}'$ ( $10^{-29} \text{ cm}^2 \text{ keV}$ )
$^{123}\text{Te}$	$1.0 \pm 0.5$	$< 60 \pm 20$
	$2.8 \pm 0.2$	$2000 \pm 300$
	$4.2 \pm 0.2$	$7000 \pm 1000$
$^{125}\text{Te}$	$4.2 - 4.5$	$7000 \pm 3000$

The neutron flux was measured with standard activation techniques<sup>12</sup> by the inclusion of indium foils in the target stacks. Each disk was 0.0127 cm thick with a diameter of 3.8 cm and a mass of about 1 g. Epithermal neutrons were observed by detection of the 416.92-keV fluorescence from the 54.15-min isomer of <sup>116</sup>In, which is produced through neutron capture from the stable <sup>115</sup>In. At the highest photon end point of 6 MeV, there were found to be only  $0.87 \pm 0.05$  neutrons  $\text{cm}^{-2} \text{s}^{-1}$ , and this flux decreased smoothly to zero as the end point was lowered to the deuterium ( $\gamma, n$ ) threshold of 2.22 MeV. This low level of epithermal neutron flux produced negligible contributions to the yields of <sup>123,125</sup>Te<sup>m</sup> and <sup>87</sup>Sr<sup>m</sup>. The appearance of thermal neutrons was not expected because of the lack of sufficient moderators in the environment. The use of photon energies below the thresholds of all target and environmental materials excluded fast neutron production.

### CONCLUSIONS

The excitation functions obtained in this work for the population of the isomers <sup>125</sup>Te<sup>m</sup> and <sup>125</sup>Te<sup>m</sup> indicate that their photoexcitation proceeds through absorption by isolated intermediate states. No consistent description could be obtained by assuming absorption through densely spaced levels which would have provided broadband

absorption. The integrated cross sections determined for these states are about 100 times larger than most ( $\gamma, \gamma'$ ) activation reactions reported previously, being in excess of  $10^{-26} \text{ cm}^2 \text{ keV}$ . Moreover, they are only an order of magnitude smaller than those determined in earlier measurements<sup>1,5</sup> for the depopulation of <sup>180</sup>Ta<sup>m</sup>. Clearly, further investigations of the systematics of isomeric photoexcitation are needed in the range between 2 MeV and ( $\gamma, n$ ) threshold energies in order to isolate the principal cause of the large photoexcitation rates being found. Experimental studies of a variety of different isomeric nuclei are currently underway to examine these questions. It would also be of great interest to have nuclear structure calculations illuminating the nature of the particular intermediate states through which the photoabsorption occurs.

### ACKNOWLEDGMENTS

We thank K. Alrutz-Ziemssen, H.-D. Gräf, Th. Rietdorf, and H. Weise for their great support in operating the superconducting electron accelerator. In addition, we wish to thank our sponsors, the Department of Defense through the Naval Research Laboratory and the Bundesministerium für Forschung und Technologie, Contract No. 06DA184I.

<sup>1</sup>C. B. Collins, C. D. Eberhard, J. W. Glesener, and J. A. Anderson, *Phys. Rev. C* **37**, 2267 (1988).

<sup>2</sup>J. J. Carroll, J. A. Anderson, J. W. Glesener, C. D. Eberhard, and C. B. Collins, *Astrophys. J.* **344**, 454 (1989).

<sup>3</sup>Zs. Nemeth and F. Kaeppler, contribution to the Symposium on Nuclear Astrophysics, Baden, 1990 (unpublished).

<sup>4</sup>C. B. Collins, F. W. Lee, D. M. Shemwell, B. D. DePaola, S. Olariu, and I. I. Popescu, *J. Appl. Phys.* **53**, 4645 (1982).

<sup>5</sup>C. B. Collins, J. J. Carroll, T. W. Sinor, M. J. Byrd, D. G. Richmond, K. N. Taylor, M. Huber, N. Huxel, P. v. Neumann-Cosel, A. Richter, C. Spieler, and W. Ziegler, *Phys. Rev. C* **42**, 1813 (1990).

<sup>6</sup>J. J. Carroll, M. J. Byrd, D. G. Richmond, T. W. Sinor, K. N. Taylor, W. L. Hodge, Y. Paiss, C. D. Eberhard, J. A. Anderson, C. B. Collins, E. C. Scarbrough, P. P. Antich, F. J. Agee, D. Davis, G. A. Huttlin, K. G. Kerris, M. S. Litz, and D. A. Whittaker, submitted to *Phys. Rev. C*.

<sup>7</sup>H.-D. Gräf and A. Richter, in Proceedings of the 1988 Linear Accelerator Conference, Virginia, CEBAF Report No. 89-001, 1989, p. 231.

<sup>8</sup>E. Browne and R. B. Firestone, in *Table of Radioactive Isotopes*, edited by V. S. Shirley (Wiley, New York, 1986).

<sup>9</sup>Walter R. Nelson, Hideo Hirayama, and David W. O. Rogers, *The EGS 4 Code System* (SLAC Report No. 265, Stanford Linear Accelerator Center, Stanford, CA, 1985).

<sup>10</sup>R. Mohan, C. Chui, and L. Lidofsky, *Med. Phys.* **12**, 595 (1985).

<sup>11</sup>*Monte Carlo Transport of Electrons and Photons*, edited by T. M. Jenkins, Walter R. Nelson, and Alessandro Rindi (Plenum, New York, 1988).

<sup>12</sup>*ASTM Standard Method for Determining Thermal Neutron Reaction and Fluence Rates by Radioactivation Techniques*, Publication E 262-86 (American Society for Testing and Materials, Philadelphia, 1987), and references cited there.